Recent Research in Science and Technology 2014, 6(1): 78-82
ISSN: 2076-5061
Available Online: http://recent-science.com/

Kinetics and mechanisms of ciprofloxacin cleavage in light assisted fenton reaction

Ardhendu Sekhar Giri[1] and Animes Kumar Golder[2]

Department of Chemical Engineering, Indian Institute of Technology Guwahati, Assam- 781039, India
.

Abstract
Ciprofloxacin (CIP) is a broad-spectrum antibacterial drug of fluoroquinolone class. The activity of CIP should vanish through transformation of piperazine and fluorine substituents Fenton reaction. The objective of the present study was to compare the kinetics of degradation and mineralization of CIP in light assisted Fenton reaction. The batch experiment was performed in presence of a low pressure UV lamp of 9 W at wavelength of 362 nm with 400 mL 15 mg/L CIP solution in a 1 L photo-reactor at 25°C. The molar ratio of Fe^{2+}/H_2O_2 and pH were chosen as 0.125 and pH 3.5 from the experimental optimization of CIP decomposition studies. Maximum drug and mineralizing efficiency were of 97.4 and 84.1%. The rate of drug mineralization was about 5 times slower than that of CIP cleavage. Mass spectra displayed that 11 intermediates were originated upon CIP oxidation in Fenton reaction with UV irradiation. The degradation mechanism suggested that most of the intermediates were attached to the core quinolone structure.

Keywords: Fluoroquinolone, Photo-Fenton, Mineralization, Hydroxyl radical, Degradation mechanism.

INTRODUCTION

Pharmaceuticals present in liquid as well as in solid wastes are recognized as an emerging group of contaminants [1]. Many studies confirm their presence in various aquatic sources namely, surface water, sewage treatment plant (STP) effluents, seawater and groundwater [2]. They enter into the environment primarily from municipal and industrial effluents, water treatment plant sludge, manure from animal husbandry and agricultural runoff. Antibacterial medicines are employed to treat infections caused by bacteria. It inhibits bacterial growth or kills them. Antibiotics also have been widely used as growth promoters in animal farming [3]. Ciprofloxacin (CIP) belongs to fluoroquinolone class of antibiotic drugs. It works against both gram-positive and gram-negative bacteria. CIP obstructs the catalytic cycle of important enzymes for nucleic acid synthesis of the bacteria [4]. CIP has been detected in hospital effluents very commonly in the range from 11 to 99 µg/L [5], in STP influent even upto 0.14 µg/L [5] and in raw drinking water upto 0.032 µg/L [6]. Hydroxyl radicals ($OH^{\bullet}$) have already ratified their efficiency to cause non-selectivity decomposition of different classes of pharmaceuticals even found at low concentrations [7]. The most effective method of hydroxyl radicals ($OH^{\cdot}$) formation is photo-assisted Fenton process. Light causes photolysis of $[Fe(OH)]^{2+}$ and additional $OH^{\bullet}$ radicals are generated (Eq. (1)). Furthermore, UV light can induce photodegradation of some intermediates such as Fe(III)-carboxylate complexes (Eq. (2)). The process uses ferrous salts and hydrogen peroxide at ambient temperature and pressure under UV or solar radiation [8].

*Corresponding Author

Ardhendu Sekhar Giri
Department of Chemical Engineering, Indian Institute of Technology Guwahati, Assam- 781039, India

Email: a.giri@iitg.ernet.in

$$Fe(OH)^{2+} + hv \longrightarrow Fe^{2+} + OH^{\bullet} \quad (1)$$

$$Fe(OOCR)^{2+} + hv \longrightarrow Fe^{2+} + CO_2 + R^{\bullet} \quad (2)$$

In this study, the performance photo-Fenton process (PFP) for the decomposition of CIP from aqueous solution and its mineralization under an optimal condition is investigated. A mechanistic path for CIP oxidation is proposed and supported by the compounds appeared in LC-MS spectra.

EXPERIMENTAL

Analytical technique

HPLC instrument of M/s Simadzu (Model: 26462, Japan) equipped with UV-visible detector was employed for the chromatographic measurement of concentration of CIP. Acetonitrile (98% v/v purity), water and tri-ethylamine (98% v/v purity) at the flow rate of 1 mL/min (20:80:0.1 v/v/v) was used as the mobile phase. Liquid chromatography-time-of-flight mass spectrometry (LC-TOF-MS) (Waters Q-Tof Premier & Aquity UPLC) system was used for the detection of reaction fragments. An YMC Hydrosphere C_{18} 150 mm×4.6 mm reverse phase analytical column (Wilmington, NC, US) following an YMC Hydrosphere 10 mm×4 mm guard column was employed. The mobile phase consisting of H_2O and acetonitrile with 0.1% (v/v) formic acid was run at 0.8 mL/min flow rate. Total organic carbon (TOC) analyzer was employed for determination of TOC before and after experiments (M/s O.I. Analytical (Model: 1030C Aurora, USA). Solution pH was read using a pH meter (model: pH/ion 510) of M/s Eutech Instruments (Malaysia).

Reagents and solution preparations

HPLC grade CIP (purity >98%) was procured from M/s Sigma Aldrich Chemical Ltd (USA). The chemical structure of CIP is illustrated in Figure 1. HPLC grade of methanol (purity 98%), ferrous ammonium sulphate hexahydrate (99% purity, w/w), sulphuric acid

(98% purity), sodium hydroxide (98% purity) and H_2O_2 (50% purity) were obtained from M/s Merck Specialties Pvt Ltd (India).

Experimental procedure

A batch reactor of a one litre capacity cylindrical (Ø 105 mm) borosilicate vessel was used. The experiment was performed at room temperature (23-25°C) with 400 mL drug solution. 0.05N H_2SO_4 was used to adjust the pH of the solution. Predetermined amount of Fe^{2+} and H_2O_2 was then added followed by illumination of UV light. 0.1 N NaOH was added immediately to stop the reaction at 10:1 (v/v). The clear supernatant was analysed for pH, drug concentration, TOC and LC-MS spectra.

RESULTS AND DISCUSSION

Drug removal and Mineralisation

Degradation of CIP by UV-Fenton was investigated with addition of both Fe^{2+} and H_2O_2. Removal of CIP showed two distinct rate periods (Figure 2) i.e. initial faster drug removal followed by almost invariant rate period. Within first 5 min, $OH^{\bullet}$ concentration falls down very quickly and then it decreases gradually. The net rate of $OH^{\bullet}$ production with progress of reaction time is resulted from the combined effect of H_2O_2 scavenging by H^+ and H_2O_2 photolysis forming additional $OH^{\bullet}$ radicals (Eq. (3)) [9]. Figure 2 also shows the variation of TOC reduction with the progress of reaction. CIP degradation was faster than mineralization and 97.4% CIP was decomposed in 45 min with 10 mM H_2O_2. TOC removal was about 13.3% lesser within 45 min of irradiation. Whereas, only a slight decrease in CIP (8.3%) and TOC (5.2%) were observed after 45 min of illumination in case of direct UV photolysis.

$$H_2O_2 + h\nu \rightarrow 2OH^{\bullet} \ (k = 3.3\times10^7\ M^{-1}s^{-1}) \qquad (3)$$

Proposed mechanisms of CIP degradation

Eleven degradation products were identified in the mass spectra obtained at 10 min of light aided Fenton reaction (Figure 3). The primary CIP degradation reactions molecule include (a) photooxidation, (b) defluorination and, (c) cleavage of piperazine ring (Figure 4). The acid-base characteristics of CIP molecule is influenced by the physicochemical properties of the solvent due to present of carboxyl and amine groups [10]. The two pK_a values of CIP of 6.8 and 8.9 are due to O-H bond ionization and N-H bond breaking [11]. Deprotonation of N_4 in piperazine ring is typically the preferred site for $OH^{\bullet}$ attack [12]. Whereas, N_1 is probably less reactive than N_4 because of its weaker basicity [13]. The aromatic ring contains two strong electron-withdrawing nitrogen substituents i.e. -F and -COOH groups (Figure 1).

On the other hand, highly electron-withdrawing fluorine substituent makes the fluoroquinolone ring less electron-donating in nature [10]. Generally, the loss of fluoride ($[M+H-22]^+$) and carboxyl moiety ($[M+H-44]^+$) are the typical decomposition routes of fluoroquinolone [14]. The formation of daughter ions could follow three pathways for the degradation of CIP. They are piperazine moiety degradation, defluorination and decarboxylation. The possible pathways CIP molecule cleavages are illustrated in Figure 4. The peaks in the mass spectra with m/z of 305, 304, 239, 304, 301, 287, 186, 205, 198, 217 and 242 were for the retention time of 5.36 min (Figure 3). The symbol 'D' denotes the degradation products following an integer to count the number. The fragment D_1 with m/z 305 has the same specific mass of 7-[2-amino-ethyl) amino]-6-fluoroquinoline formed by the loss of piperazine ring under acidic conditions (Figure 4a). The fragmentations with m/z of 304, 239 and 304 (D_2 to D_4) appeared from D_1 molecule. D_2 and D_4 molecules have the same mass (m/z) number but they formed in different routes. D_2 was originated by partial piperazine ring breaking followed by hydroxylation of D_1 (Figure 4a). D_4 was produced by decarboxylation and subsequent hydroxylation of CIP molecule. They were formed through the common mechanistic pathway of piperazine ring breakage.

D_3 was yielded by piperazine ring cleavage and defluorination of D_2. D_4 molecule appeared from D_1 via an intermediate having m/z of 287.1, by decarboxylation and defluorination. Piperazine ring under goes an angle stress in presence of high electronegative fluorine atom of this intermediate. All fragments of CIP except D_1 (m/z= 305) were decarboxylated products. MS spectra of the compound D_1 denotes a fragment of CIP which might be originated by the loss of piperazine moiety rather than decarboxylation [11]. D_5 (m/z=301) was defluorinated and hydroxylated product of D_4 molecule. Dehydroxylation of D_1 led to formation of D_6 (m/z 287) (Figure 4b). D_7 (m/z= 186), D_8 (m/z= 205), D_9 (m/z= 198), D_{10} (m/z= 217) and D_{11} (m/z= 242) fragment were produced due to cleavage of N-C bond of cyclic amine ring and by subsequent protonation and hydroxylation. Partial breakage of piperazine ring followed by defluorination of D_6 gave D_7 molecule.

D_8 molecule having m/z 205 was formed by hydroxylation of D_7 and protonation thereafter. The electrophilic substitution reaction is enhanced by electron donating ability of cyclic amine attached to quinolone moiety. Cleavage of cyclic amine ring of D_7 molecule caused D_9 (m/z = 198) appearance. Hence cyclic amine group was broken out due to an angle strain [12]. D_{10} with m/z of 217 was formed by hydroxylation through homolytic cleavage of π-bond of D_9 followed by hydroxylation and protonation. Also an electrophilic substitution reaction is increased by electron donating ability of aliphatic amine chain attached to quinolone moiety. Further, D_{11} molecule having m/z of 242 was originated by partial breaking of piperazine moiety of D_1 and successive defluorination. Six membered piperazine ring suffers more angle strain. The proposed pathway(s) and structure of the intermediates are summarized in Table 1.

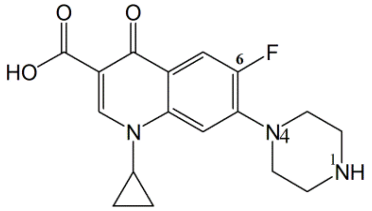

Fig 1. Chemical structure of Ciprofloxacin (CIP) drug.

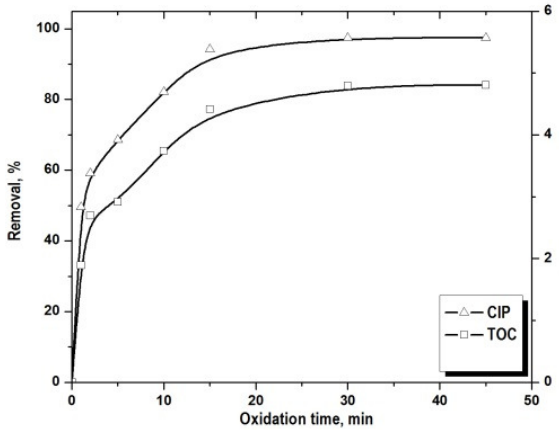

Fig 2. CIP and TOC removal with reaction time. Experimental conditions: $[CIP]_0$=15mg/L, $[Fe^{2+}/H_2O_2]_0$ = 0.125 mM, pH = 3.5, UV = 9W and temperature =25°C.

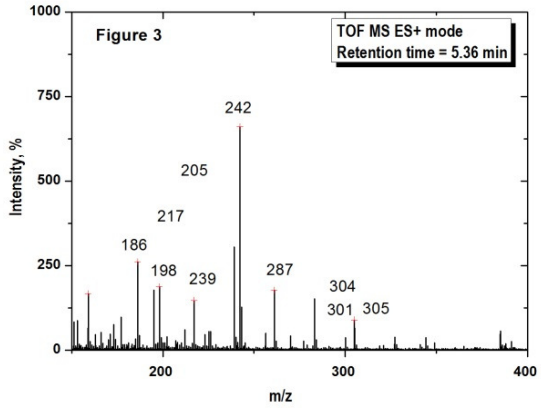

Fig 3. Mass spectra of CIP degradation recorded at 10 min of UV illumination. Experimental conditions: $[CIP]_0$ =15mg/L, $[Fe^{2+}/H_2O_2]_0$ = 0.125 mM, pH = 3.5, UV = 9 W and temperature =25°C.

Figure 4a

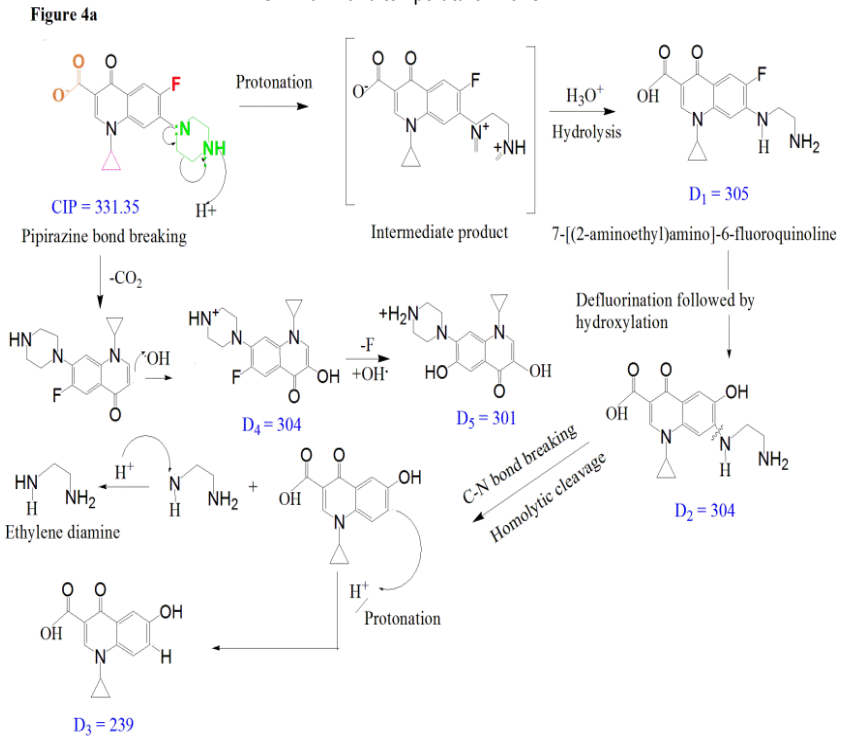

Fig 4a.

Figure 4b

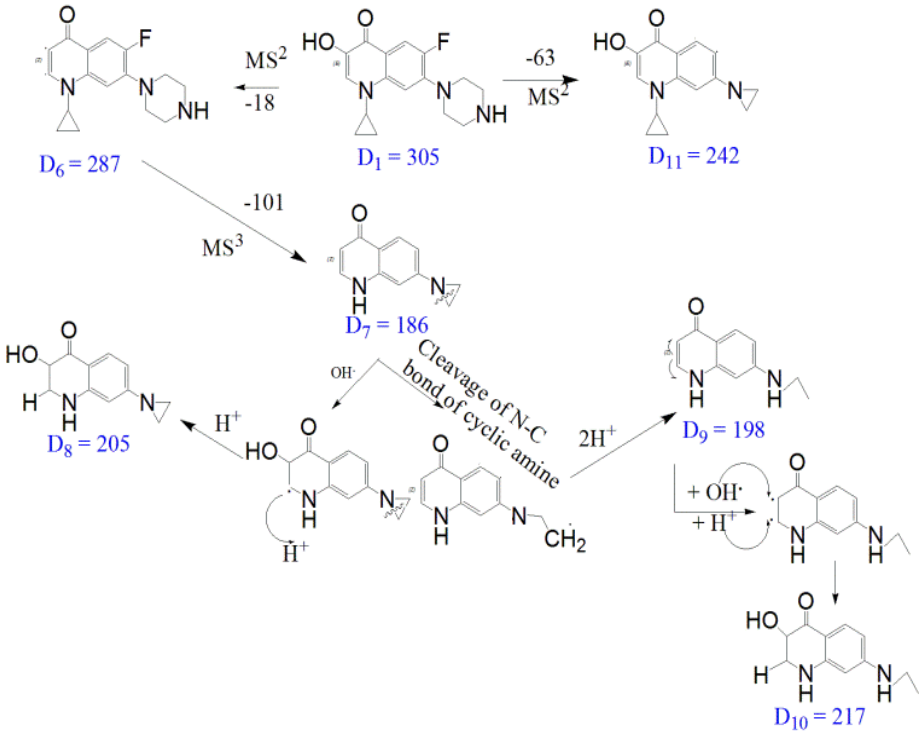

Fig 4b.

Fig 4 (a). Proposed mechanisms for the formation of daughter ions on degradation of CIP. (b) Continued from D1. Mass spectra of CIP degradation recorded at 10 min of UV illumination. Experimental conditions: $[CIP]_0$=15mg/L, $[Fe^{2+}/H_2O_2]_0$ = 0.125 mM, pH = 3.5, UV = 9W and temperature =25°C.

Table 1. The pathway(s) and proposed structure of daughter ions of CIP formed in PFP.

Daughter ions	Molecular Formula	m/z (MH^+)	Degradation route
D_1	$C_{15}H_{16}O_3N_3F$	305	Partial piperazine ring cleavage
D_2	$C_{14}H_{14}O_4N_3F$	304	Defluorination followed by Hydroxylation of D_1
D_3	$C_{14}H_{14}O_4N$	239	Piperazine ring breaking followed by defluorination of D_1
D_4	$C_{11}H_{10}ON_3F$	304	Decarboxylation followed by hydroxylation of D_1
D_5	$C_{11}H_{12}ON_3$	301	Decarboxylation followed by hydroxylation of D_1
D_6	$C_{11}H_{12}ON_2$	287	Decarboxylation of D_1
D_7	$C_{11}H_{10}O_2N_2$	186	Partial piperazine ring cleavage of D_6
D_8	$C_{11}H_{10}O_2N_2$	205	Partial piperazine ring cleavage followed by hydroxylation of D_7
D_9	$C_{11}H_{10}O_2N_2$	198	Decarboxylation followed by partial piperazine ring breaking of D_1
D_{10}	$C_{11}H_{10}O_2N_2$	217	Decarboxylation followed hydroxylation of D_1
D_{11}	$C_{11}H_{10}O_2N_2$	242	Decarboxylation followed by hydroxylation of D_1

CONCLUSIONS

The present results demonstrated that CIP removal of 97.4% was noted with $[CIP]_0$ =15 mg/L at pH = 3.5 and Fe^{2+}/H_2O_2 molar ratio 0.125. TOC removal was 84.1%. A large numbers of intermediates were resistant to oxidation due to refractory nature of quinolone moiety. Eleven primary daughter ions appeared in the mass spectra acquired at 10 min of UV-light assisted Fenton reaction. The first intermediate with m/z of 305 was yielded by piperazine moiety degradation. Whereas, the rests were originated through decarboxylation, defluorination and hydroxylation. Piperazine moiety degradation was more effective due to an angle strain influenced by fluorine atom.

REFERENCES

[1] R. Alexy, T. Kümpel, K. Kümmerer, 2002. Biodegradability of some antibiotics, elimination of the genotoxicity and affection of wastewater bacteria in a simple test. *Chemosphere* 57:505-512.

[2] T.A. Ternes, 1998. Occurrence of drugs in German sewage treatment plants and rivers. *Water Res.* 32:3245-3260.

[3] L. Gunnarsson, E. Kristiansson, C. Rutgersson, J. Sturve, J. Fick, L. Forlin, D.G.J. Larsso, 2009. Effluent from drug manufacturing affects cytochrome P450 1 regulation and function in fish. *Environ. Toxicol. Chem.* 28 (12):2639-2647.

[4] L. Gao, Y. Shi, W. Li, H. Niu, J. Liu, Y. Cai, 2012. Tetracycline oxidation and growth inhibition. *Chemosphere* 86:665-671.

[5] B. Morasch, F. Bonvin, H. Reiser, D. Grandjean, L.F. de Alencastro, C. Perazzolo, N. Chèvre, T. Kohn, 2010. Occurrence and fate of micropollutants in the Vidy Bay of Lake Geneva, Switzerland. Part II: Micropollutant removal between wastewater and raw drinking water. *Environ. Toxicol. Chem.* 29:1658-1668.

[6] J. Hofmann, U. Freier, M. Wecks, S. Hohmann, 2007. Degradation of diclofenac in molecularly imprinted polymer submicron particles by UV light irradiation and HCl acid treatment. *Applied Catal. B: Environ.* 70:447-451.

[7] S.A.S. Melo, A.G. Trovo, I.R. Bautitz, R.F.P. Nogueira, 2009. Treatment of effluent from a factory of paints using solar photo-Fenton process. *Química Nova* 32:188-197.

[8] P. Wang, Y.L. He, C.H. Huang, Degradation of residual pharmaceuticals by advanced oxidation processes. *Water Res.* 44 (2010) 5989-5998.

[9] M. Klavarioti, D. Mantzavinos, D. Kassinos, 2009. Treatment of dairy wastewater by inorganic coagulants: Parametric and disposal studies. *Environ. Int.* 35:402-417.

[10] Z. Wang, K Chen, J, Li. L. Mo., Q. Wang, 2008. Environmental applications using graphene composites: water remediation and gas adsorption, Nanoscale. *Environ. Int.,* 22:211-216.

[11] H. Park, H.T. Kim, K. Bark, 2002. Synthesis, characterisation and biological activity of novel 4-thiazolidinones, 1,3,4-oxadiazoles. *Eur. J. Med. Chem.* 37:443-448.

[12] H. Tekin, O. Bilkay, S. Selale, H. Tolga, 2006. Use of Fenton oxidation to improve the biodegradability of a pharmaceutical wastewater. *J. Hazard. Mater.* 136:258-265.

[13] M. Hesse, H. Meier, B. Zeeh, "Spectroscopic Methods in Organic Chemistry" 2nd ed., Thieme, New York.

[14] D. Klauson, J. Babkina, K. Stepanova, M. Krichevskaya, S. Preis, 2010. Photocatalytic oxidation of organic pollutants in aqueous and gaseous phases. *Catal. Today,* 151:39-45.